Pulsed-Gradient Spin−Echo 1H and 19F NMR Ionic Diffusion Coefficient, Viscosity, and Ionic Conductivity of Non-Chloroaluminate Room-Temperature Ionic Liquids

ARTICLE *in* THE JOURNAL OF PHYSICAL CHEMISTRY B · APRIL 2001

Impact Factor: 3.3 · DOI: 10.1021/jp004132q

3 AUTHORS, INCLUDING:

Kikuko Hayamizu
University of Tsukuba
195 PUBLICATIONS **7,266** CITATIONS
SEE PROFILE

Masayoshi Watanabe
Yokohama National University
350 PUBLICATIONS **14,344** CITATIONS
SEE PROFILE

Pulsed-Gradient Spin−Echo ^{1}H and ^{19}F NMR Ionic Diffusion Coefficient, Viscosity, and Ionic Conductivity of Non-Chloroaluminate Room-Temperature Ionic Liquids

Akihiro Noda,[†] Kikuko Hayamizu,[‡] and Masayoshi Watanabe*,[†]

Department of Chemistry and Biotechnology, Yokohama National University, 79-5 Tokiwadai, Hodogaya-ku, Yokohama 240-8501, Japan, and National Institute of Materials and Chemical Research, 1-1 Higashi, Tsukuba 305-8565, Japan

Received: November 9, 2000; In Final Form: March 5, 2001

Room-temperature ionic liquids, 1-ethyl-3-methylimidazolium tetrafluoroborate ($EMIBF_4$), 1-ethyl-3-methylimidazolium bis(trifluoromethylsulfonyl)imide (EMITFSI), 1-butylpyridinium tetrafluoroborate ($BPBF_4$), and 1-butylpyridinium bis(trifluoromethylsulfonyl)imide (BPTFSI), were prepared and characterized. The thermal property, density, self-diffusion coefficient of the anions and cations, viscosity, and ionic conductivity were measured for these ionic liquids in wide temperature ranges. A pulsed-gradient spin−echo NMR method was used to independently measure self-diffusion coefficients of the anions (^{19}F NMR) and the cations (^{1}H NMR). The results indicate that the cations diffuse almost equally to the anion in $EMIBF_4$ and $BPBF_4$, whereas they diffuse faster than the anion in EMITFSI and BPTFSI. The summation of the cationic and anionic diffusion coefficients for each ionic liquid follows the order EMITFSI > $EMIBF_4$ > BPTFSI > $BPBF_4$, under an isothermal condition. The order of the magnitude of the diffusion coefficient well contrasts with that of the viscosity for each ionic liquid. The temperature dependencies of the self-diffusion coefficient, viscosity, and ionic conductivity obey the Vogel−Tamman−Fulcher (VTF) equation, and the VTF parameters were presented. Relationships among the self-diffusion coefficient, viscosity, and molar conductivity were analyzed in terms of the Stokes−Einstein equation and the Nernst−Einstein equation. The most interesting feature of the relationships is that the ratios of the molar conductivity, determined by complex impedance measurements, to that calculated from the NMR diffusion coefficients, range from 0.6 to 0.8 for $EMIBF_4$ and $BPBF_4$, whereas the ratios range from 0.3 to 0.5 for EMITFSI and BPTFSI. This difference could be understood by taking the ionic association into consideration for EMITFSI and BPTFSI.

Introduction

After the first discovery of non-chloroaluminate room-temperature ionic liquids by Wilkes,[1] many room temperature ionic liquids have been extensively explored. At present, it is known that certain combinations of organic cations, such as imidazolium and pyridinium derivatives, and bulky and soft anions, such as PF_6^-, BF_4^-, $CF_3SO_3^-$, and $(CF_3SO_2)_2N^-$, form ionic liquids at near room temperature.[2−5] The characteristics of these ionic liquids are, for instance, chemical and thermal stability, nonvolatility, nonflammability, high ionic conductivity, and a wide electrochemical potential window. Various trials have been made to have a fundamental understanding of these ionic liquids and to introduce them in practical applications, such as batteries, capacitors, and electrochemical solar cells.[6−14] The formation of polymer electrolytes based on these ionic liquids has also been proposed,[15−17] and furthermore, polyelectrolytes having polymerized structures of these molten salts have been investigated.[18−20] However, the fundamental understanding of the ionic transport properties is not sufficient. For example, the ionic diffusion coefficient, the degree of ionic association, and the interaction between ions have not been clearly revealed. Because the ionic liquids are concentrated electrolyte solutions, interpretations of their transport properties are very complicated.

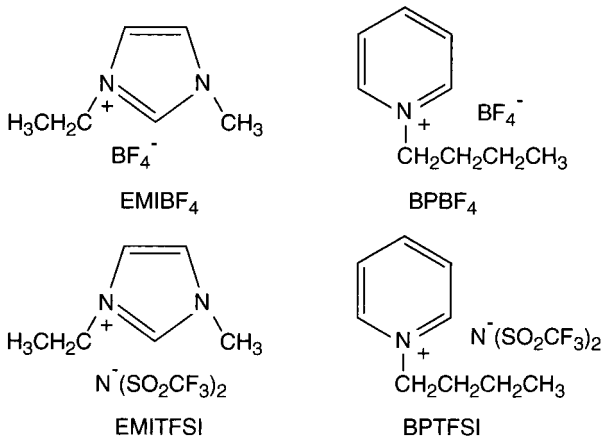

Figure 1. Molecular structures of $EMIBF_4$ EMITFSI, $BPBF_4$, and BPTFSI.

We present here experimental results of the thermal property, density, self-diffusion coefficient, viscosity, and ionic conductivity for 1-ethyl-3-methylimidazolium tetrafluoroborate ($EMIBF_4$), 1-ethyl-3-methylimidazolium bis(trifluoromethylsulfonyl)imide (EMITFSI), 1-butylpyridinium tetrafluoroborate ($BPBF_4$), 1-butylpyridinium, and bis(trifluoromethylsulfonyl)imide (BPTFSI) (see Figure 1). The temperature dependencies of the self-diffusion coefficient of the anions (^{19}F NMR) and the cations (^{1}H NMR), determined by using pulsed-gradient spin−echo NMR (PGSE-NMR) technique, viscosity, and ionic conductivity,

* To whom correspondence should be addressed. E-mail: mwatanab@ynu.ac.jp. Fax: +81-45-339-3955.
[†] Yokohama National University.
[‡] National Institute of Materials and Chemical Research.

10.1021/jp004132q CCC: $20.00
Published on Web 04/26/2001

are fitted with the Vogel−Tamman−Fulcher (VTF) equation, and the obtained parameters are presented and compared with each other. The molar conductivity calculated from the self-diffusion coefficients of ionic liquids and the Nernst−Einstein equation are compared with the experimental molar conductivity calculated from the ionic conductivity and the density. These results indicate the presence of the ionic association or the ionic components that cannot contribute to ionic conduction, especially in the ionic liquids having TFSI as their anion.

Experimental Section

Synthesis. 1-Ethyl-3-methylimidazolium chloride and 1-butylpyridinium chloride were synthesized according to the procedure described in earlier publications.[17,21] The anion exchange reaction to form $EMIBF_4$ and $BPBF_4$ was made by using $AgBF_4$ (Aldrich) in ethanol/water,[1,3,17] and that to form EMITFSI and BPTFSI was carried out using LiTFSI (kindly supplied by IREQ) in water by metathesis reaction.[4,5] The ionic liquids were dehydrated under high vacuum, and the structure of each ionic liquid was identified by ^1H NMR and fast atom bombardment mass spectra. These ionic liquids were stored in an argon atmosphere glovebox (VAC, $[O_2] < 1$ ppm, $[H_2O] < 1$ ppm).

Thermal Property. Differential scanning calorimetry (DSC) was carried out by using a Seiko Instruments DSC 220C under N_2 atmosphere. The samples for DSC measurements were tightly sealed in Al pans. Thermograms were recorded during cooling (373−123 K) scans, followed by heating (123−373 K) scans at a cooling and heating rate of 10 K min^{-1}. The glass transition temperature (T_g, onset of the heat capacity change), crystallization temperature (T_c), and melting temperature (T_m) were determined from DSC thermograms during the heating scans. High-temperature stabilities for the ionic liquids were measured on a Seiko Instruments thermo-gravimetry/differential thermal analyzer (TG/DTA 6200) from 303 to 773 K at a heating rate of 10 K min^{-1} under N_2 atmosphere.

Density. The density measurement was conducted by using a density/specific gravity meter DA-100 (Kyoto Electronics Manufacturing Co., Ltd.). The measuring temperature range was between 293 and 313 K.

Self-Diffusion Coefficient. The PGSE-NMR measurements were made by using a JEOL GSH-200 spectrometer with a 4.7 T wide bore superconducting magnet, which is controlled by a TecMAG Galaxy system equipped with JEOL pulse field gradient probes and a current amplifier. The ^{19}F and ^1H spectra were measured with a $^{19}F/^1H$ probe. The procedure of PGSE-NMR method followed the previous publications.[22−25] The measurements of the self-diffusion coefficients for the cation and anion in each ionic liquid were made by using ^1H and ^{19}F nuclei, respectively. The simple spin−echo pulse sequence was used for the self-diffusion measurements. The echo signal attenuation, E, is related to the experimental parameters by[26]

$$\ln(E) = \ln(S/S_{g=0}) = -\gamma^2 g^2 D\delta^2(\Delta - \delta/3) \qquad (1)$$

where S is the spin−echo signal intensity, δ is the duration of the field gradient with magnitude g, γ is the gyromagnetic ratio, and Δ is the interval between the two gradient pulses. In the present experiments, the g value used was constant (5.78 T m^{-1}), the δ was in the range of 0−3.5 ms, and the Δ value used was 50 ms. A recycle delay sufficient in allowing full relaxation (i.e., $>5T_1$) was used between each transition. The ^1H diffusion coefficients were almost the same for each ^1H in the cations, and data in the present paper were obtained from the signal attenuation of the ^1H on the 3-methyl for EMI and on the terminal methyl for BP, respectively. The ^{19}F NMR exhibited one peak assigned to ^{19}F for BF_4 and TFSI. The measurements were carried out with cooling from 373 to 263 K. The samples were thermally equilibrated at each temperature for 15 min before the measurements.

TABLE 1: Thermal Properties for $EMIBF_4$, EMITFSI, $BPBF_4$, and BPTFSI

	T_g/K[a]	T_c/K[a]	T_m/K[a]	T_d/K[b]
$EMIBF_4$	184	222	288	664
EMITFSI	186	181	257	690
$BPBF_4$	202	251	272	615
BPTFSI		224	299	677

[a] Onset temperatures of a heat capacity change (T_g), an exotherm peak (T_c), and an endotherm peak (T_m) during a heating scan from 123 K by using differential scanning calorimetry. [b] Temperature of 10% weight loss during heating scan from room temperature by using thermogravimetry.

Viscosity. Viscosity of the ionic liquids was measured with a Toki RE80 cone-plate viscometer under N_2 atmosphere, and temperature control (353−273 K) was conducted with a Thomas TRL-108H circulation-type thermo-regulated bath.

Ionic Conductivity. Ionic conductivity for the ionic liquids was determined by means of the complex impedance measurements with stainless-steal blocking electrodes, using a computer controlled Hewlett-Packard 4192A LF impedance analyzer over the frequency range from 5 Hz to 13 MHz. A sample was filled between mirror-finished stainless steel electrodes using a Teflon ring spacer (13 mm outer diameter, 7 mm inner diameter, 2 mm thickness) and was sealed in a Teflon container in the glovebox.[27] The measurements were carried out with cooling from 373 to 263 K by using a Yashima BX-10 thermostated oven, and the samples were thermally equilibrated at each temperature for at least 1 h before the measurements.

Results and Discussion

DSC and Density. Thermal properties for the ionic liquids were studied using DSC. During cooling from 373 to 123 K at 10 K min^{-1}, only a heat capacity change corresponding to the glass transition could be observed for $EMIBF_4$ and $BPBF_4$. It means that the crystallization rates of both of the ionic liquids are very slow and that the supercooled liquids are fairly stable.[15,16] For instance, $EMIBF_4$ did not crystallize at 213 K for more than 5 h and $BPBF_4$ did not crystallize at 243 K for more than 7 h. In contrast, an exothermic peak based on the crystallization and a heat capacity change assigned to the glass transition were observed for EMITFSI and BPTFSI during the cooling scans, indicating relatively fast crystallization rates of these ionic liquids. In the following heating scans, the thermograms showed T_g, T_c, and T_m, successively, for most of the ionic liquids.[12] The DSC results and the thermal stability, determined by thermo-gravimetry, are summarized in Table 1.[28] The ionic liquids, investigated in this study, have wide liquid temperature ranges together with high thermal stability. Especially, EMITFSI[5,12] and BPTFSI exhibit higher thermal stability than $EMIBF_4$ and $BPBF_4$.

Table 2 shows the temperature dependence of density. In this range of temperature from 293 to 313 K, the density decreases linearly with the temperature increase, irrespective of the ionic liquid structures. The density values lower and higher than this temperature range were calculated by extrapolating the linear temperature dependence. On the basis of the density data and

TABLE 2: Density and Molar Concentration for $EMIBF_4$, EMITFSI, $BPBF_4$, and BPTFSI[a]

	$EMIBF_4$	EMITFSI	$BPBF_4$	BPTFSI
T/K	$\rho/10^6$ g m^{-3}	$\rho/10^6$ g m^{-3}	$\rho/10^6$ g m^{-3}	$\rho/10^6$ g m^{-3}
313	1.266	1.502	1.208	1.436
308	1.271	1.507	1.212	1.440
303	1.275	1.512	1.216	1.444
298	1.279	1.518	1.220	1.449
293	1.283	1.523	1.224	1.453

	$EMIBF_4$	EMITFSI	$BPBF_4$	BPTFSI
T/K	$M/10^3$ mol m^{-3}	$M/10^3$ mol m^{-3}	$M/10^3$ mol m^{-3}	$M/10^3$ mol m^{-3}
313	6.39	3.84	5.42	3.45
308	6.42	3.85	5.43	3.46
303	6.44	3.86	5.45	3.47
298	6.46	3.88	5.47	3.48
293	6.48	3.89	5.49	3.49

[a] Molecular wt./g mol^{-1}; $EMIBF_4$ 197.97; EMITFSI 391.32; $BPBF_4$ 223.01; BPTFSI 416.36.

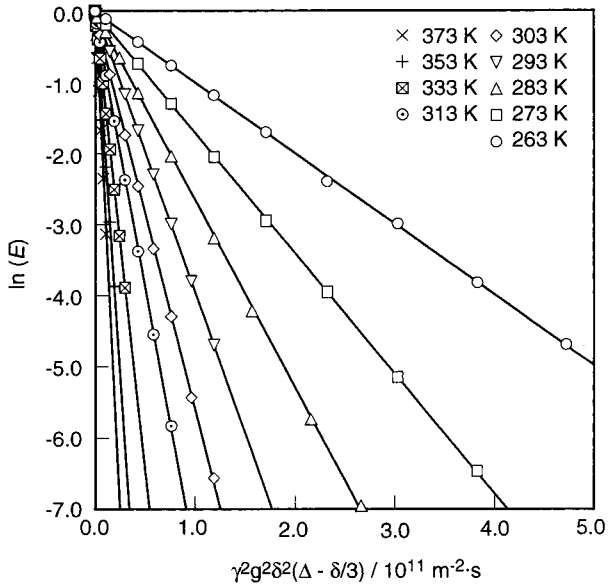

Figure 2. Plots of signal attenuation versus $\gamma\ ^2g^2\delta\ ^2(\Delta - \delta/3)$ for ^{1}H PGSE-NMR echo signals of $EMIBF_4$. In this experiment, $g = 5.78$ Tm^{-1}, δ ranged from 0 to 3.5 ms, and Δ was 50 ms.

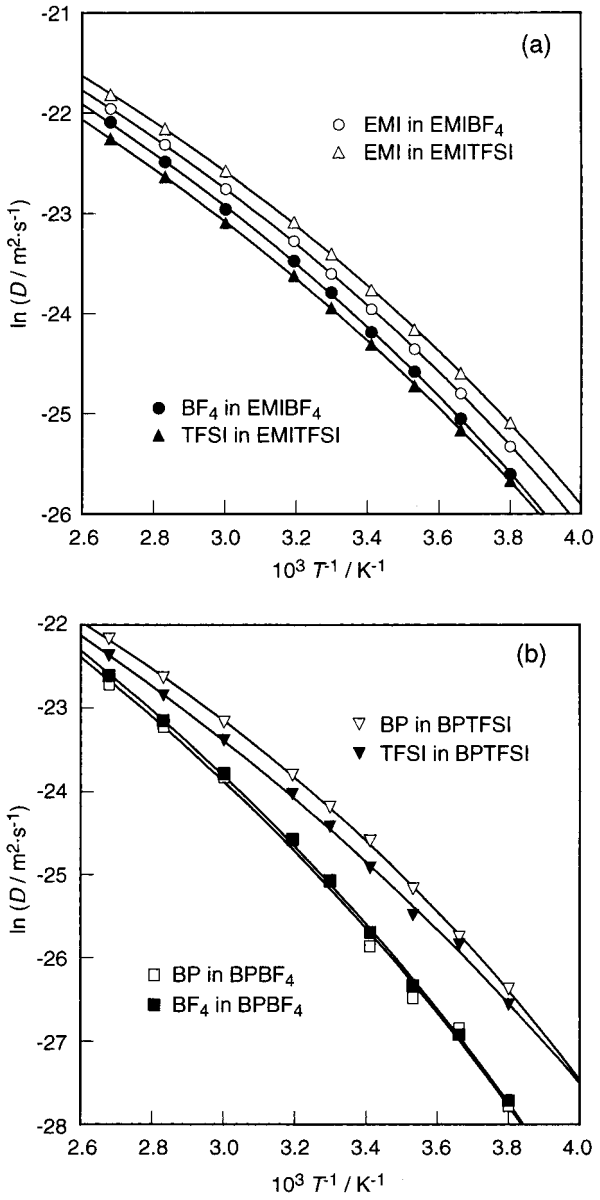

Figure 3. Arrhenius plots of self-diffusion coefficients of anion and cation for (a) $EMIBF_4$ and EMITFSI and for (b) $BPBF_4$ and BPTFSI.

the molecular weight, the molar concentration of each ionic liquid was calculated and is listed in Table 2.

Self-Diffusion Coefficient and Its Correlation with Viscosity. The PGSE-NMR method is noninvasive and makes it possible to independently measure the self-diffusion coefficient of each ionic species in the system under the study, provided that the components contain NMR sensitive nuclei.[22−25] In this measurement, ^{19}F and ^{1}H were used for detecting for the anions and the cations, respectively. Figure 2 exhibits one of the results of PGSE-NMR measurements (the relationship between left-hand term and right-hand term in eq 1). Each set of the result shows good linear relationship, and the self-diffusion coefficient can be obtained from the slope of each set of plots and eq 1. Although the linearity of the plots (see Figure 2) is consistent with the measured species in the fast exchange limit in the time scale of Δ (50 ms), the measured species, that is, each ion, interacts with each other. Because Coulombic attractive force between the anions and the cations is strong, the ions would associate to form ion pairs and ion aggregates. However, Coulombic repulsive force also exists. Thus, the equilibrium of the attractive and repulsive interaction at each temperature, keeping the charge valance, relates to the chemical equilibrium for association and dissociation of the components in the ionic liquids. Because NMR measurement detects a nucleus (i.e., ^{1}H or ^{19}F) and cannot distinguish between the ion and their associated species, the PGSE-NMR diffusion coefficients obtained in this experiment seem to be an average self-diffusion coefficient of the ions and associated ions. In addition, because the signal splitting between the ions and their aggregates was not observed, the rate of exchange constants between the ions and ion aggregates are shorter than the NMR time scale.

Arrhenius plots of the apparent self-diffusion coefficient of the cation (D_{cation}) and anion (D_{anion}) for $EMIBF_4$ and EMITFSI and for $BPBF_4$ and BPTFSI are depicted in Figure 3 parts a and b, respectively. The summation ($D_{cation} + D_{anion}$) of the cationic and anionic diffusion coefficients is shown in Figure 4 also as Arrhenius plots. Temperature dependency of each set of the self-diffusion coefficients show convex curved-profiles; therefore, each result of the self-diffusion coefficient is fitted with the Vogel−Tamman−Fulcher (VTF) equation[29]

$$D = D_0 \exp[-B/(T - T_0)] \qquad (2)$$

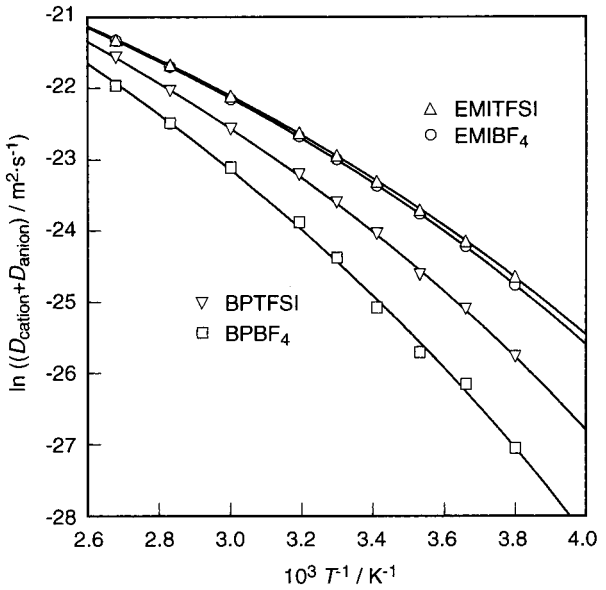

Figure 4. Arrhenius plots of simple summation of cationic and anionic self-diffusion coefficients ($D_{cation} + D_{anion}$) for $EMIBF_4$, EMITFSI, $BPBF_4$, and BPTFSI.

TABLE 3: VTF Equation Parameters for Apparent Self-Diffusion Coefficient Data

$D = D_0 \exp[-B/(T - T_0)]$

	$D_0/10^{-8}$ m^2 s^{-1}	$B/10^2$ K	$T_0/10^2$ K	$R^2/10^{-1}$
		$EMIBF_4$		
cation	1.6	9.7	1.3	9.99
anion	1.6	10	1.3	9.99
cation + anion	3.3	9.9	1.3	9.99
		EMITFSI		
cation	1.7	9.4	1.3	9.99
anion	1.7	11	1.2	9.99
cation + anion	3.3	9.9	1.3	9.99
		$BPBF_4$		
cation	6.9	15	1.3	9.99
anion	7.8	15	1.3	9.99
cation + anion	15	15	1.3	9.99
		BPTFSI		
cation	2.5	11	1.4	9.99
anion	5.3	14	1.2	9.99
cation + anion	6.6	12	1.3	9.99

where D_0 (m^2 s^{-1}), B (K), and T_0 (K) are constants. The solid lines in Figures 3a,b and 4 are drawn based on the VTF equation and the best-fit parameters. The best-fit parameters of the VTF equation for these ionic liquids are summarized in Table 3. Apparent cationic transference numbers ($D_{cation}/(D_{cation} + D_{anion})$) are shown in Figure 5 to compare the self-diffusion coefficients between the anion and the cation. For $EMIBF_4$ and $BPBF_4$, the cationic diffusion coefficients are similar to the anionic diffusion coefficient. When the anion is replaced by more bulky TFSI, the relative diffusivity of the cations to that of the anion becomes larger and the VTF B parameters of the cation become smaller than those of the TFSI anion (Table 3). The comparison of B parameters between the ionic liquids with the EMI cation and those with the BP cation indicates that larger activation energies (larger B values) are required for the ionic liquids with the BP cation. The differences of the D_0 and T_0 parameters between the cation and the anion are small, and especially, T_0 parameters are ca. 1.3×10^2 K for all of the ionic liquids. These results reveal that the differences of the ionic self-diffusion coefficient at each temperature are mainly dependent on the B parameters, that is, the activation energies.

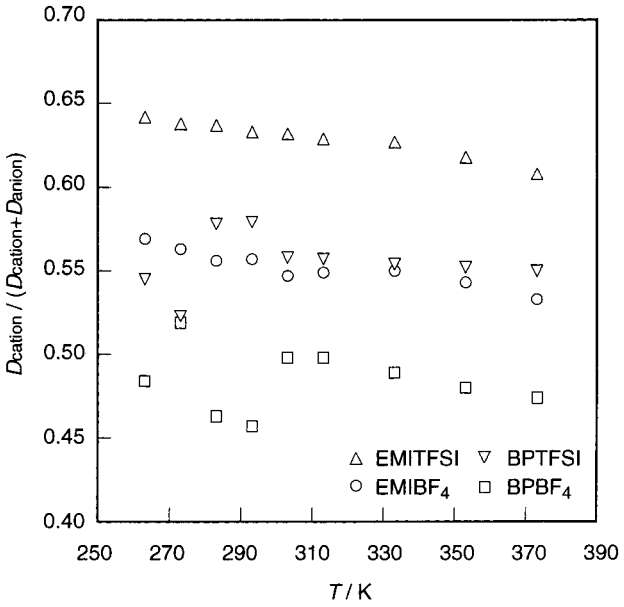

Figure 5. Temperature dependence of apparent cationic transference number for $EMIBF_4$, EMITFSI, $BPBF_4$, and BPTFSI.

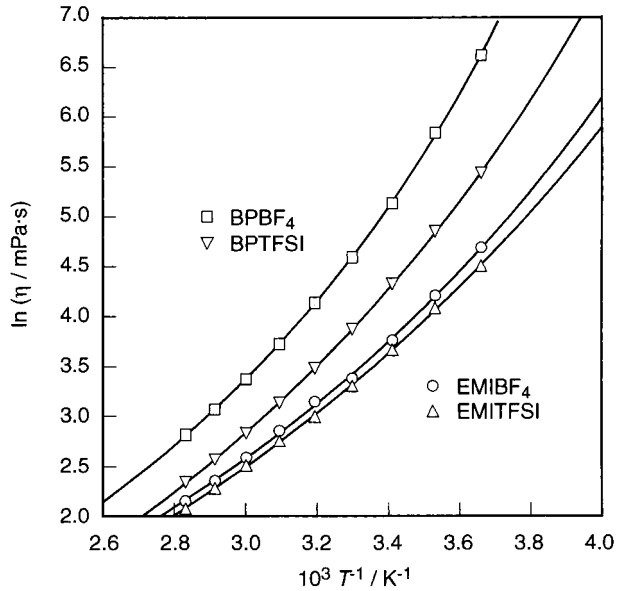

Figure 6. Arrhenius plots of viscosity for $EMIBF_4$, EMITFSI, $BPBF_4$, and BPTFSI.

TABLE 4: VTF Equation Parameters for Viscosity Data

$\eta = \eta_0 \exp[B/(T - T_0)]$

	$\eta_0/10^{-1}$ mPa s	$B/10^2$ K	$T_0/10^2$ K	$R^2/10^{-1}$
$EMIBF_4$	2.0	7.5	1.5	9.99
EMITFSI	1.5	8.4	1.4	9.99
$BPBF_4$	2.3	7.2	1.8	9.99
BPTFSI	1.2	8.5	1.6	9.99

Arrhenius plots of the viscosity for the ionic liquids and their VTF fitting curves are shown in Figure 6. The VTF equation is

$$\eta = \eta_0 \exp[B/(T - T_0)] \quad (3)$$

where η_0 (mPa s), B (K), and T_0 (K) are constants. The VTF parameters of viscosity are listed in Table 4. The measured temperature dependency of the viscosity for $EMIBF_4$ and EMITFSI agrees well with the data reported by McEwen et al.[12] and Bonhôte et al.[5]

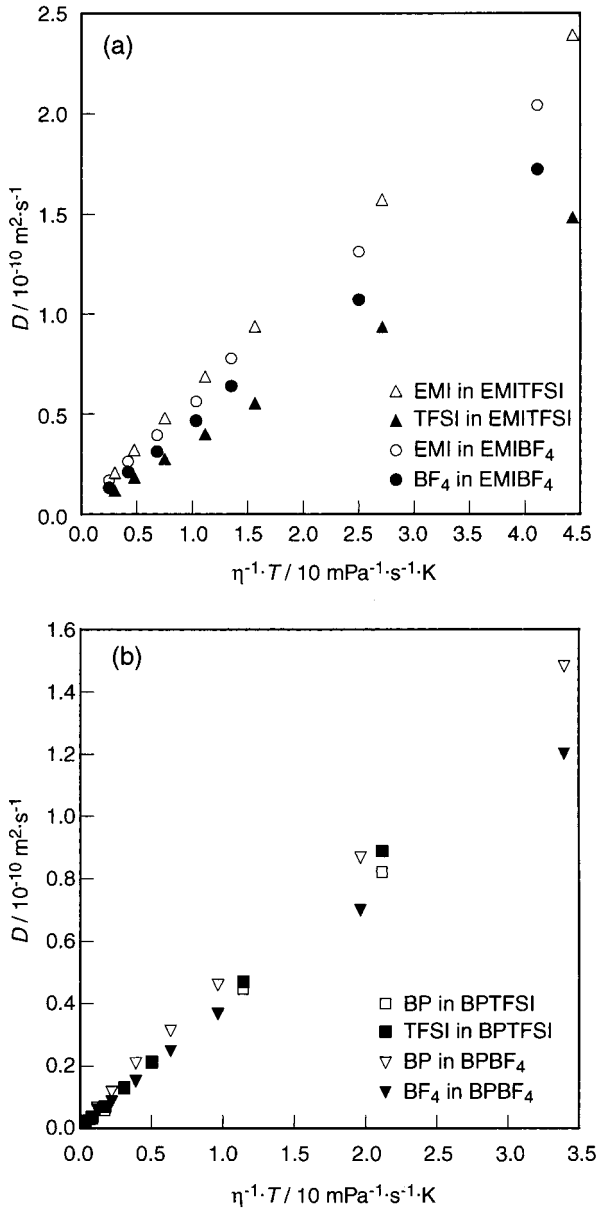

Figure 7. Relationship between T/η (T, absolute temperature; η, viscosity) and self-diffusion coefficients of the anion and cation for (a) $EMIBF_4$ and EMITFSI and for (b) $BPBF_4$ and BPTFSI.

The results of temperature dependencies of the viscosity (Figure 6) and the summation of the self-diffusion coefficient ($D_{cation} + D_{anion}$; Figure 4) are well contrasted with each other. Thus, the correlation between the self-diffusion coefficient (D_{cation} and D_{anion}) and viscosity (η) is considered by using the Stokes−Einstein equation:

$$D = kT/c\pi\eta r \tag{4}$$

where k is the Boltzmann constant, T is the absolute temperature, c is a constant (4−6), and r is effective hydrodynamic or Stokes radius. The relationships between the self-diffusion coefficient of the anion (D_{anion}) and the cation (D_{cation}) and T/η for $EMIBF_4$ and EMITFSI, and for $BPBF_4$ and BPTFSI, are depicted in Figure 7 parts a and b, respectively. All of the relationships in Figure 7a,b can be approximated by linear lines, indicating that the ionic diffusivity in the ionic liquids basically obeys eq 4. However, it is soon understood that the slopes of the relationships do not reflect the size of each ionic species. As shown in Figure 7a, EMI cation in EMITFSI and $EMIBF_4$ indicated

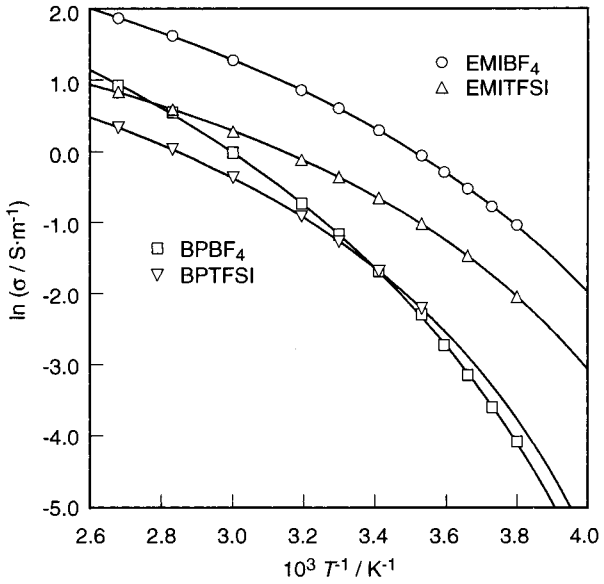

Figure 8. Arrhenius plots of ionic conductivity for $EMIBF_4$, EMITFSI, $BPBF_4$, and BPTFSI.

similar and the largest slopes in the relationships, followed by the BF_4 anion and the TFSI anion. If these results are explained by using eq 4, the hydrodynamic radius of each ion follows the order TFSI > BF_4 > EMI and does not reflect the calculated ion size by McEwen et al.[12] Figure 7b indicates that the BP cation, TFSI anion, and BF_4 anion have a similar hydrodynamic radius, irrespective of the difference in the calculated ion size. Because the ionic liquids are highly concentrated electrolyte solutions (Table 2), an ion in the liquids may diffuse dependently with each other. The influence of Coulombic interaction between ionic species, i.e., attractive and repulsive interaction, and the equilibrium between dissociated ions and associated ions also seem to be important for understanding the relation between the ionic size and the diffusivity. The previous study by Hussey et al. shows the importance of the ionic charge effect which affects the transport properties.[30] This paper indicates that the increase of overall negative anionic charge of metal complexes increases the relative hydrodynamic radii in chloroaluminate- or bromoaluminate-ionic liquids. Furthermore, it is very interesting that the monomeric and polymeric anions exhibit almost the same hydrodynamic radii, if their overall negative charge is the same. However, the ionic liquids we used consist of only monocharged anions and cations. Our data of the apparent cationic transference number shows that the cation diffuses a little faster than the anion, except for $BPBF_4$. In addition, the results of the Stokes−Einstein relationships (Figure 7) show the cationic hydrodynamic radii are relatively smaller than the both of TFSI and BF_4 anions in our ionic liquids. If considering the calculated BF_4 hydrodynamic radius, this should be smaller than the EMI and BP radius. Consequently, the cation diffuses more easily than the anion. The delocalization of cationic charge, owing to their resonance ring structures, would be important.

Molar Conductivity and Its Correlation with Diffusion Coefficient. Figure 8 exhibits the temperature dependence of the ionic conductivity, determined by complex impedance measurements, and their VTF fitting curves. The VTF equation is

$$\sigma = \sigma_0 \exp[-B/(T - T_0)] \tag{5}$$

where σ_0 (Sm^{-1}), B (K), and T_0 (K) are constants. The best VTF fitting parameters are given in Table 5. The results of the

TABLE 5: VTF Equation Parameters for Ionic Conductivity Data

$\sigma = \sigma_0 \exp[-B/(T - T_0)]$

	$\sigma_0/10^1$ S m^{-1}	$B/10^2$ K	$T_0/10^2$ K	$R^2/10^{-1}$
$EMIBF_4$	6.7	4.6	1.8	9.99
EMITFSI	1.6	3.6	1.9	9.99
$BPBF_4$	8.6	6.6	1.9	9.99
BPTFSI	1.5	4.1	2.0	9.99

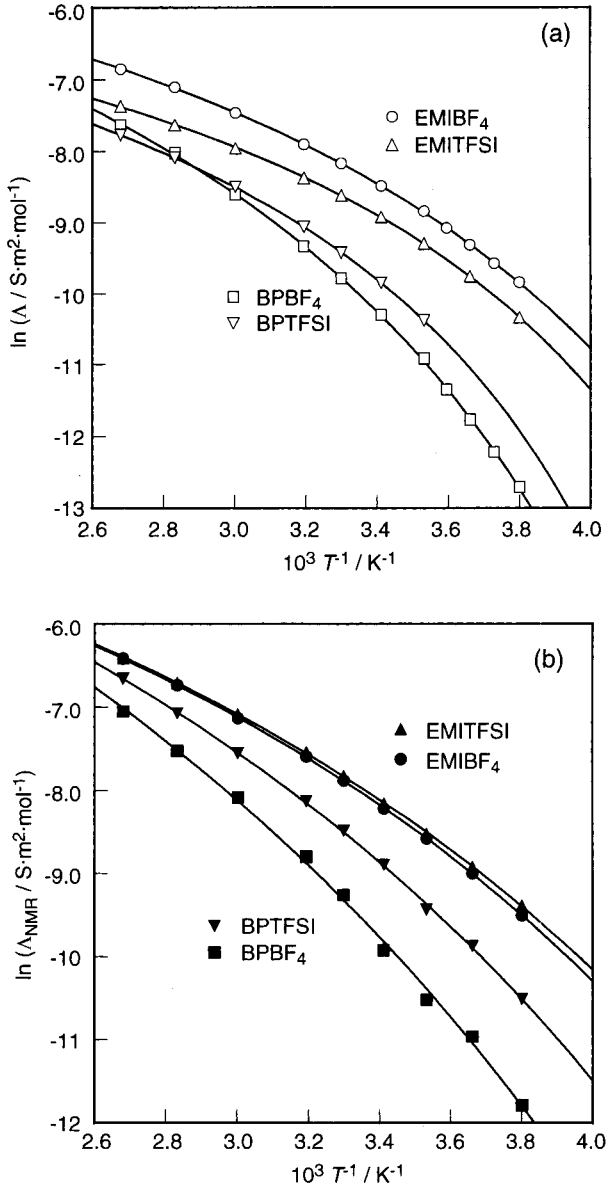

Figure 9. Arrhenius plots of molar conductivity for $EMIBF_4$, EMITFSI, $BPBF_4$, and BPTFSI (a) Λ obtained experimentally from conductivity and molar concentration and (b) Λ_{NMR} calculated from ionic self-diffusion coefficients and the Nernst−Einstein equation.

ionic conductivity for $EMIBF_4$ and EMITFSI agree with those reported by McEwen et al.[12] Molar conductivity of the ionic liquids was calculated from the ionic conductivity and the molar concentration. The temperature dependency of the molar conductivity and their VTF fitting curves are shown in Figure 9a. The VTF equation is

$$\Lambda = \Lambda_0 \exp[-B/(T - T_0)] \quad (6)$$

where Λ_0 (Sm^{-2} mol^{-1}), B (K), and T_0 (K) are constants. The best VTF fitting parameters are listed in Table 6.

TABLE 6: VTF Equation Parameters for Molar Conductivity Data

$\Lambda = \Lambda_0 \exp[-B/(T - T_0)]$

	$\Lambda_0/10^{-3}$ S m^{-2} mol^{-1}	$B/10^2$ K	$T_0/10^2$ K	$R^2/10^{-1}$
$EMIBF_4$	13	5.0	1.7	9.99
EMITFSI	4.9	3.9	1.9	9.99
$BPBF_4$	19	6.8	1.8	9.99
BPTFSI	5.0	4.3	2.0	9.99

$\Lambda_{NMR} = \Lambda_0 \exp[-B/(T - T_0)]$

	$\Lambda_0/10^{-2}$ S m^{-2} mol^{-1}	$B/10^2$ K	$T_0/10^2$ K	$R^2/10^{-1}$
$EMIBF_4$	4.5	7.6	1.4	9.99
EMITFSI	4.5	7.6	1.4	9.99
$BPBF_4$	20	13	1.4	9.97
BPTFSI	9.2	9.9	1.4	9.99

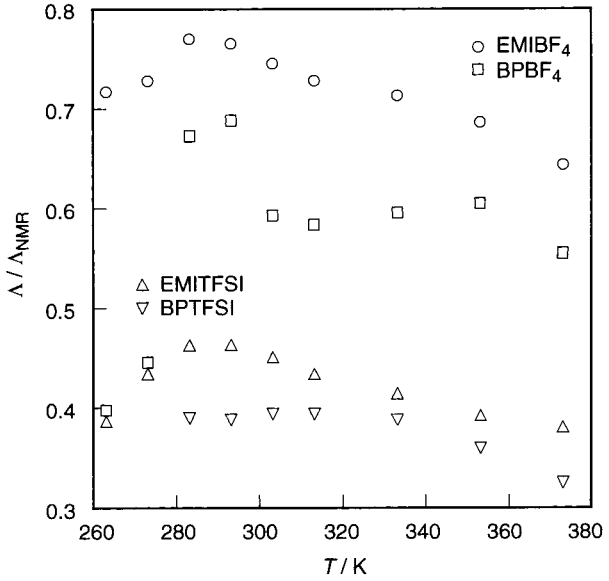

Figure 10. Molar conductivity ratios (Λ/Λ_{NMR}) plotted against temperature for $EMIBF_4$, EMITFSI, $BPBF_4$, and BPTFSI.

The Nernst−Einstein equation is applied to calculate molar conductivity (Λ_{NMR}) from the PGSE-NMR diffusion coefficients:

$$\Lambda_{NMR} = N_A e^2 (D_{cation} + D_{anion})/kT = F^2 (D_{cation} + D_{anion})/RT \quad (7)$$

where N_A is the Avogadro's number, e is electric charge on each ion, F is the Faraday's constant, and R is the gas constant. Arrhenius plots of the estimated molar conductivity (Λ_{NMR}) are shown in Figure 9b, and their best VTF fitting parameters are shown in Table 6. By comparing the experimental molar conductivity (Λ) to the calculated molar conductivity (Λ_{NMR}), it can be noticed that the Λ values are lower than the Λ_{NMR} values at each temperature in the measured temperature range. The ratios (Λ/Λ_{NMR}) are, thus, plotted against temperature, as shown in Figure 10. The Nernst−Einstein equation is derived without considering ionic association and is also derived on the assumption that each ion has the activity of unity. Thus, the Λ/Λ_{NMR} ratios give us the information about the ionic association and/or the ionic activity in the ionic liquids. As can be seen from Figure 10, the Λ/Λ_{NMR} ratios range from 0.6 to 0.8 for $EMIBF_4$ and $BPBF_4$, whereas the ratios range from 0.3 to 0.5 for EMITFSI and BPTFSI. The ratio of Λ/Λ_{NMR} indicates the percentage of ions, which can contribute to ionic conduction in the diffusion components. Thus, we can estimate the fraction of the ion pairs or aggregations by $(1 - \Lambda/\Lambda_{NMR})$. However,

as mentioned above, NMR cannot distinguish between the ions and ion aggregates. Also, as already pointed out, their exchange rate is faster than the NMR time scale. In this case, the measured results are average, and the percentage of ions or aggregations are also "time-averaged ion" or "time-averaged aggregations", as "time-averaged solvation", which was suggested by Hussey et al.[30] We recognize that we can define the percentage of the ions as the existence probability, if we can measure NMR and conductivity on the same time scale.

The relatively large Λ/Λ_{NMR} values indicate that the ionic liquids basically consist of charged cationic and anionic species, which can diffuse and contribute to the ionic conduction. Especially for $EMIBF_4$ and $BPBF_4$, the Λ/Λ_{NMR} ratios are high enough to assume that these ionic liquids consist of the ions, that the NMR diffusion coefficients reflect the individual ionic diffusivity, and that most of the ions contribute to the ionic conduction. In other words, the activity of each ion is close to unity. The situation might not be so straightforward and become a little complicated in EMITFSI and BPTFSI. The Λ/Λ_{NMR} ratios are evidently smaller than those for $EMIBF_4$ and $BPBF_4$. The summation of the self-diffusion coefficient ($D_{cation} + D_{anion}$) at each temperature (Figure 4) follows the order EMITFSI > $EMIBF_4$ > BPTFSI > $BPBF_4$, which reflects the magnitude of the viscosity (Figure 6). However, the high diffusivity for EMITFSI and BPTFSI is not reflected in their molar conductivity (Figure 9a). This is a direct reason for the small Λ/Λ_{NMR} ratios. The viscosity of the ionic liquids seems to be affected by many molecular parameters, such as molecular weight and shape of each ion and Coulombic interaction between the ionic species. If looking at the difference in the viscosity between the ionic liquids with the EMI cation and with the BP cation, the larger cationic size and the larger cationic molecular weight may cause a larger viscosity of the latter ionic liquids. The effect of molecular weight on the viscosity is no more valid for the viscosity values when considering the anionic structures. Although the formula weight of the TFSI anion is much larger than that of the BF_4 anion, the viscosity of the ionic liquids with the TFSI anion is lower than that of the BF_4 anion. One possible reason for this is the presence of ion-pairs and neutral ion aggregates in the ionic liquids with the TFSI anion, which dilutes the ionic concentration and reduces Coulombic interaction between the ionic species. The reduced Coulombic interaction may decrease the viscosity, which in turn enhances the ionic diffusion coefficient. However, the ion pairs and neutral ion aggregates cannot contribute to the ionic conduction, and thus, the molar conductivity of the ionic liquids with TFSI anion becomes small. Certain molecular interaction between the cations and the TFSI anion, for instance, a hydrogen bonding interaction, might play an important role in understanding the low Λ/Λ_{NMR} ratios for the EMI ionic liquids with TFSI anion. However, there is no evidence of hydrogen bonds involving the BP cation. Finally, it could be pointed out from Figure 10 that the Λ/Λ_{NMR} ratios do not vary much with temperature, though the data is rather scattered. This might imply that the structure of each ionic liquid does not greatly change with temperature.

Conclusions

The PGSE-NMR method is used to independently measure the self-diffusion coefficients of the anions (^{19}F NMR) and the cations (^1H NMR) in the ionic liquids. Temperature dependencies of the self-diffusion coefficient, viscosity, and ionic conductivity for $EMIBF_4$, EMITFSI, $BPBF_4$, and BPTFSI do not obey the Arrhenius equation; however, they obey the VTF equation, instead. The summation of the cationic and the anionic diffusion coefficients for each ionic liquid is well correlated with the inverse of the viscosity. The apparent cationic transference number in $EMIBF_4$ and $BPBF_4$ is close to 0.5, and it increases to some extent when the anion is replaced by the more bulky TFSI anion. The size of each ion does not directly affect the ionic diffusion coefficient. The Nernst−Einstein equation is applied to understand the correlation between the ionic diffusion coefficient and the molar conductivity. The ratios of the experimental molar conductivity by complex impedance measurements to the calculated molar conductivity from the NMR diffusion coefficient range from 0.6 to 0.8 for $EMIBF_4$ and $BPBF_4$, whereas the ratios range from 0.3 to 0.5 for EMITFSI and BPTFSI. The smaller ratios for EMITFSI and BPTFSI are caused by the facts that the summation of the cationic and the anionic diffusion coefficients is larger for the ionic liquids with the TFSI anion, whereas the experimental molar conductivity becomes larger for the ionic liquids with the BF_4 anion. The ionic association in EMITFSI and BPTFSI could be a reason for this phenomenon.

Acknowledgment. This research was supported in part by a Grant-in-Aid for Scientific Research on Priority Areas of "Molecular Synchronization for Design of New Materials System (#404/11167234)" from the Japanese Ministry of Education, Culture, Sports, Science and Technology and by NEDO International Joint Research Grant.

References and Notes

(1) Wilkes, J. S.; Zaworotko, M. J. *J. Chem. Soc., Chem. Commun*. **1992**, 965.
(2) Fuller, J.; Carlin, R. T.; De Long, H. C.; Haworth, D. *J. Chem. Soc., Chem. Commun*. **1994**, 299.
(3) Carlin, R. T.; De Long, H. C.; Fuller, J.; Trulove, P. C. *J. Electrochem. Soc*. **1994**, *141*, L73.
(4) Koch, V. R.; Nanjunduah, C.; Appetecchi, G. B.; Scrosati, B. *J. Electrochem. Soc*. **1995**, *142*, L116.
(5) Bonhôte, P.; Dias, A.-P.; Papageorgiou, N.; Kalyanasundaram, K.; Grätzel, M. *Inorg. Chem*. **1996**, *35*, 1168.
(6) Koch, V. R.; Dominey, L. A.; Nanjundiah, C. *J. Electrochem. Soc*. **1996**, *143*, 798.
(7) Croce, F.; D'Aprano, A.; Nanjundiah, C.; Koch, V. R.; Walker, C. W.; Salmon, M. *J. Electrochem. Soc*. **1996**, *143*, 154.
(8) Papageorgiou, N.; Athanassov, Y.; Armand, M.; Bonhôte, P.; Pettersson, H.; Azam, A.; Grätzel, M. *J. Electrochem. Soc*. **1996**, *143*, 3099.
(9) McEwen, A. B.; McDevitt, S. F.; Koch, V. R. *J. Electrochem. Soc*. **1997**, *144*, L84.
(10) Nanjundiah, C.; McDevitt, S. F.; Koch, V. R. *J. Electrochem. Soc*. **1997**, *144*, 3392.
(11) Fuller, J.; Carlin, R. T.; Osteryoung, R. A. *J. Electrochem. Soc*. **1997**, *144*, 3881.
(12) McEwen, A. B.; Ngo, H. L.; LeCompte, K.; Goldman, J. L. *J. Electrochem. Soc*. **1999**, *146*, 1687.
(13) Every, H.; Bishop, A. G.; Forsyth, M.; MacFarlane, D. R. *Electrochim. Acta* **2000**, *45*, 1279.
(14) Doyle, M.; Choi, S. K.; Proulx, G. *J. Electrochem. Soc*. **2000**, *147*, 34.
(15) Fuller, J.; Breda, A. C.; Carlin, R. T. *J. Electrochem. Soc*. **1997**, *144*, L67.
(16) Fuller, J.; Breda, A. C.; Carlin, R. T. *J. Electroanal. Chem*. **1998**, *459*, 29.
(17) Noda, A.; Watanabe, M. *Electrochim. Acta* **2000**, *45*, 1265.
(18) Ohno, H.; Ito, K. *Chem. Lett*. **1998**, 751.
(19) Hirao, M.; Ito, K.; Ohno, H. *Electrochim. Acta* **2000**, *45*, 1291.
(20) Ito, K.; Nishina, N.; Ohno, H.; *Electrochim. Acta* **2000**, *45*, 1295.
(21) Wilkes, J. S.; Levinsky, L. A.; Wilson, R. A.; Hussey, C. L. *Inorg. Chem*. **1982**, *21*, 1263.
(22) Hayamizu, K.; Aihara, Y.; Arai, S.; Price, W. S. *Solid State Ionics* **1998**, *107*, 1.
(23) Hayamizu, K.; Aihara, Y.; Arai, S.; Martinez, C. G. *J. Phys. Chem. B* **1999**, *103*, 519.

(24) Hayamizu, K.; Aihara, Y.; Arai, S.; Price, W. S. *Electrochim. Acta* **2000**, *45*, 1313.
(25) Aihara, Y.; Arai, S.; Hayamizu, K. *Electrochim. Acta* **2000**, *45*, 1321.
(26) Stejskal, E. O. *J. Chem. Phys*. **1965**, *43*, 3597.
(27) Kato, Y.; Watanabe, M.; Sanui, K.; Ogata, N. *Solid State Ionics* **1990**, *40*/*41*, 632.
(28) Mutch, M. L.; Wilkes, J. S. In *Molten salts XI*; Trulove, P. C., De Long, H. C., Staford, G. R., Deki, S., Eds.; The Electrochemical Society Proceedings Series: Pennington, NJ, 1998; PV 98−11, 254.
(29) Vogel, H. *Phys. Z.* **1921**, 22, 645. Fulcher, G. S. *J. Am. Ceram. Soc.* **1923**, *8*, 339.
(30) Hussey, C. L.; Sun, I.-W.; Strubinger, S. K. D.; Barnard, P. A. *J. Electrochem. Soc*. **1990**, *137*, 2515.